EUROFUSION WPHCD-PR(16) 14915

D Yordanov et al.

How does a probe inserted into the discharge influence the plasma structure?

Preprint of Paper to be submitted for publication in
Journal of Applied Physics

This work has been carried out within the framework of the EUROfusion Consortium and has received funding from the Euratom research and training programme 2014-2018 under grant agreement No 633053. The views and opinions expressed herein do not necessarily reflect those of the European Commission.

How does a probe inserted into the discharge influence its structure?

D. Yordanov, St. Lishev, and A. Shivarova

Faculty of Physics, Sofia University, BG-1164 Sofia, Bulgaria

Electronic mail: ashiva@phys.uni-sofia.bg

Abstract. Shielding the bias applied to the probe by the sheath formed around it and determination of parameters of unperturbed plasmas are in the basis of the probe diagnostics. The results from a two-dimensional model of a discharge with a probe inserted in it show that the probe influences the entire discharge structure. The increase (although slight) of the electron temperature, due to the increased losses of charged particles on the additional wall in the discharge (mainly the probe holder) leads to redistribution of the plasma density and plasma potential, as shown by the results obtained at the floating potential of the probe. The deviations due to the bias applied to the probe tip are stronger in the ion saturation region of the probe characteristics. The pattern of the spatial redistribution of the plasma parameters advances together with the movement of the probe deeper in the discharge. Although probe characteristics and probe sheaths are shown, the study does not aims at discussions on the theories for determination of the plasma density from the ion saturation current. Regardless of the modification of the entire discharge structure, the deviations in the spatial distribution of the plasma parameters at the position of the probe tip and, respectively, the uncertainly which should be added as an error when the accuracy of the probe diagnostics is estimated, do not exceed 10%. Consequently, the electron density and temperature obtained, respectively, at the position of the plasma potential on the probe characteristics and from its transition region are in reasonable agreement with the results from the model of the discharge without a probe. Being in the scope of research on a source of negative hydrogen ions with the design of a matrix of small radius inductive discharges, the model is of a low-pressure hydrogen discharge sustained in a small-radius tube.

I. INTRODUCTION:

Probe diagnostics[1-8] is one of the most widely used tools for determination of the local values of the plasma parameters (plasma density, electron temperature and plasma potential). The methods developed for processing the probe characteristics (I-V curves presenting the dependence of the current collected by the probe on the bias applied to it, with respect to a reference electrode) involve determination of (i) the electron temperature T_e from the transition region of the probe characteristics (the region between the floating and plasma potentials, with electron motion in a retarding dc field), (ii) the plasma potential U_{pl} (from the knee in the probe characteristics between its transition region and the electron-saturation-current region or from the position of the zero value of the second derivative of the probe characteristics), and (iii) the electron density n_e from the probe current at the plasma potential or more often and even usually, from the ion saturation region (a region of ion motion in an accelerating dc field at a probe bias below the floating potential). Shielding the probe potential by ion/electron sheaths is in the basis of the concept for the probe diagnostics. Consequently, the theories for

processing the probe characteristics are based, even when they involve the Poisson equation, on description of the charged particle motion in the vicinity of the probe tip, assuming that the plasma beyond the probe sheath is not influenced by the probe bias. The discussions in the literature have not included up to now comments on the modification in the discharge structure which should be expected due to inserting the probe, with its holder, as an external body, i.e., as an additional wall inside the discharge. This requires development of a model of a discharge with a probe inserted in it, which is the aim of this study. The question which would be answered within such a model is whether or to what extent the probe diagnostics provides results for a discharge not disturbed by a probe inserted in it.

A two-dimensional (2D) fluid-plasma model of a low-pressure discharge equipped with a probe for probe diagnostics is presented. The results are compared with results from a corresponding model of a discharge not disturbed by a probe, i.e., of a discharge without a probe. An extreme situation is considered: The probe is axially movable, positioned on the axis of a small-radius discharge. Since the study is in the scope of research on a negative hydrogen ion source completed as a matrix of small-radius discharges,[9] the discharge is in a hydrogen gas.

The results discussed are for the spatial distribution of the electron density and temperature and of the plasma potential for different positions of the probe and for different values of the bias applied to its tip. The changes in the discharge structure obtained at the floating potential of the probe tip are attributed to the influence of the probe (including its holder) as a body immersed into the discharge. Due to the wall losses at the probe surface, the electron temperature increases and this leads to redistribution in the electron density and plasma potential in the entire discharge. The bias applied to the probe tip causes additional changes which, being in the opposite directions in the ion- and electron-saturation regions of the probe characteristics, are stronger in the ion saturation region. The conclusion is that the strongest changes in the discharge structure are mainly due to the probe holder. Consequently, they are in the discharge region attached to it. Moreover, the modifications in the discharge structure advance together with the movement of the probe deeper in the discharge. The deviations in the values of plasma parameters in the vicinity of the probe tip being within 3% and 5% respectively, for the electron temperature and for the plasma potential and about 10% for the electron density, are not strong. However, they should be added as an error when the accuracy of the probe diagnostics is estimated. The model properly predicts the sheath around the probe and the probe characteristics. The influence of the gas pressure on the modifications in the discharge structure is briefly commented on.

Discussions on the theories for processing the probe characteristics, in particular for determination of the electron density from the ion saturation region, are not touched. The results for the plasma parameters obtained from the probe characteristics are for the electron temperature (estimated from the transition region of the probe characteristics) and for the electron density

(estimated from the current collected by the probe at the position of the plasma potential, the latter determined from the zero value of the second derivative of the probe current). The value of the plasma parameters obtained from the probe characteristics are in reasonable agreement with those for a discharge without a probe. Part of the results has been recently presented as a conference contribution.[10]

II. DISCHARGE MODEL

A low-pressure hydrogen discharge inductively driven by a planar coil is considered. The ring-shaped power deposition Q_{ext} to the discharge is simulated with a super-Gaussian profile (Fig. 1). The plasma is sustained in a cylindrical tube with a radius of R = 2.5 cm and a length of L = 12 cm. The results presented in the next Section are without and with an axially-movable probe inserted on the discharge axis (r = 0). The probe holder is a dielectric tube with a radius of 0.3 mm. The radius of the probe tip is the same (R_{pr} = 0.3 mm) and its length is L_{pr} = 6 mm (Fig. 1). The bias applied to the probe tip has been varied (with respect to the metal discharge walls) between U_{pr} = -80 V and a value of about 10 V above the plasma potential Φ in the vicinity of the probe. The discharge ends at the metal wall like in experiments[11-13] on a single discharge of the matrix source (where the first electrode of the extraction device stops the discharge).

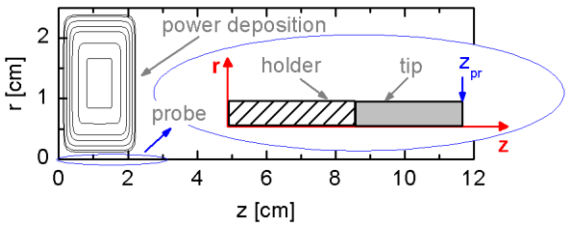

FIG. 1. The modelling domain: half of the discharge tube with the probe positioned on the discharge axis (r = 0). The rf power deposition is also shown.

The initial set of equations includes the continuity equations for electrons (α = e), positive hydrogen ions ($\alpha = j$ with j = 1,2 and 3 respectively, for the H^+, H_2^+ and H_3^+ ions) and hydrogen atoms (α = a)

$$\mathrm{div}\boldsymbol{\Gamma}_\alpha = \frac{\delta n_\alpha}{\delta t}, \tag{1}$$

the electron energy balance equation

$$\mathrm{div}\mathbf{J}_\mathrm{e} = Q_{\mathrm{ext}} + P_{\mathrm{coll}}, \tag{2}$$

the Poisson equation

$$\Delta\Phi = -\frac{e}{\varepsilon_0}\left(\sum_{j=1}^{3} n_j - n_\mathrm{e}\right) \tag{3}$$

and the equation of state

$$p = \kappa T_\mathrm{g}\left(n_\mathrm{a} + n_\mathrm{m}\right), \tag{4}$$

from which the density n_m of the molecular hydrogen is obtained.

In (1) - (4), $\mathbf{\Gamma}_\alpha$ and $\mathbf{J}_\mathrm{e}$ are, respectively, the particle and electron-energy fluxes, $\delta n_\alpha/\delta t$ and P_coll are, respectively, the particle production/losses and the electron energy losses in collisions, Φ is the plasma potential and p and T_g are, respectively, the gas pressure and the gas temperature; e, ε_0 and κ are the elementary charge, the vacuum permittivity and the Boltzmann constant.

The electron flux is a drift-diffusion flux, including also the thermal diffusion

$$\mathbf{\Gamma}_\mathrm{e} = b_\mathrm{e} n_\mathrm{e} \nabla\Phi - D_\mathrm{e}\nabla n_e - D_\mathrm{e}^\mathrm{T} n_\mathrm{e} \frac{\nabla T_\mathrm{e}}{T_\mathrm{e}} \tag{5}$$

with $b_\mathrm{e} = e/m_\mathrm{e}\nu_\mathrm{en}$, $D_\mathrm{e} = T_\mathrm{e} / m_\mathrm{e}\nu_\mathrm{en}$ and $D^T_\mathrm{e} \equiv D_\mathrm{e}$ being, respectively, the electron mobility, diffusion and thermal diffusion coefficients; T_e and n_e are the electron temperature and density, m_e is the electron mass and $\nu_\mathrm{en} = \nu_\mathrm{ea} + \nu_\mathrm{em}$ is the frequency of the elastics collisions with atoms (ν_ea) and molecules (ν_em). The rate coefficients of the latter as well as the processes of inelastic collisions in P_call and ($\delta n_\mathrm{e}/\delta t$) are for Maxwellian electron energy distribution (see Ref. 14 for more details).

The low gas pressure is specified by accounting for the inertia terms in the ion momentum equations. Consequently, the ion fluxes

$$\mathbf{\Gamma}_j = -b_j^\mathrm{eff} n_j \nabla\Phi - D_j^\mathrm{eff}\nabla n_j \tag{6}$$

include effective mobility $b_j^\mathrm{eff} = e/\left(m_j \nu_j^\mathrm{eff}\right)$ and diffusion coefficients $D_j^\mathrm{eff} = T_\mathrm{e}/\left(m_j \nu_j^\mathrm{eff}\right)$ defined with effective collision frequencies

$$\nu_j^\mathrm{eff} = \sum_{\beta=\mathrm{a,m}} \frac{m_\beta}{m_j + m_\beta} \nu_{j\beta}^\mathrm{el} + \nu_j^\mathrm{iner}. \tag{7}$$

In (6) and (7) n_j and m_j are, respectively, the density and the mass of the ions; $T_j = T_\mathrm{g}$ is their temperature. The first term in (7) accounts for the elastic ion-neutral collisions whereas the second one

$\nu^{\text{iner}}_{j(r,z)} \equiv \partial \upsilon_{(r,z)} / \partial(r,z) = -\sqrt{e/2m_j}\left(\partial_{(r,z)}\Phi / \sqrt{\Phi_{\max} - \Phi}\right)$ results from the inertia term in the ion momentum equations solved according to the approximations described in Ref. 15; for obtaining $\nu^{\text{iner}}_{j(r,z)}$ the ion energy conservation law is employed and the directions (r and z) are specified since the velocity component which is perpendicular to the given wall is that playing a role.

The flux of the hydrogen atoms is a diffusion flux:

$$\mathbf{\Gamma}_{\text{a}} = -D_{\text{a}} \nabla n_{\text{a}} , \tag{8}$$

where D_{a} is the diffusion coefficient.

The boundary conditions[16,17] for electrons and ions at the walls (the side wall (r = 2.5 cm) as well the front (z = 0) and the back (z = 12 cm) walls (Fig. 1)) are for the fluxes: $\mathbf{n}.\mathbf{\Gamma}_{\text{e}} = (1/4) n_{\text{e}} \upsilon_{\text{e,th}}$, $\mathbf{n}.\mathbf{\Gamma}_j = (1/2) n_j \upsilon_{j,\text{th}} + b_j^{\text{eff}} n_j (\mathbf{n}.\mathbf{E})$ and $\mathbf{n}.\mathbf{J}_{\text{e}}^{\text{wall}} = (5/2) T_{\text{e}} (\mathbf{n}.\mathbf{\Gamma}_{\text{e}})$; $\mathbf{n}$ is the outward unit vector, $\upsilon_{\text{e,th}}$ and $\upsilon_{j,\text{th}}$ are the thermal velocities and $\mathbf{E} = -\nabla\Phi$ is the dc electric field. The boundary conditions for the Poisson equation are: (i) a zero potential ($\Phi^{\text{wall}} = 0$) at the metal walls; (ii) equality of the electron and ion fluxes resulting in $\mathbf{n}.\nabla\Phi = [(1/2)\sum_j n_j \upsilon_{j,\text{th}} - (1/4) n_{\text{e}} \upsilon_{\text{e,th}}] / \sum_j n_j b_j^{\text{eff}}$ at the dielectric wall of the probe holder, and (iii) the bias applied to the probe tip $\Phi = U_{\text{pr}}$. At the probe tip the boundary conditions for the electron and ion fluxes are the same as at a grounded wall, for the ion when they are in an accelerating field ($\mathbf{n}.\mathbf{E} > 0$). It the opposite case the boundary condition for the ion flux is $\mathbf{n}.\mathbf{\Gamma}_j = (1/2) n_j \upsilon_{j,\text{th}}$. Axial symmetry is the boundary condition at the discharge axis (r = 0).

III. RESULTS AND DISCUSSIONS

The main results discussed are for a discharge sustained at a gas pressure p = 10 mTorr. The radius of the discharge tube is R = 2.5 cm (Fig. 1). The rf power applied for the discharge maintenance is Q_{ext} = 50 W. The axial extension of the rf power deposition region (Fig. 1) is up to z = 2.1 cm. In the discussions below U_{pl} denotes the local values of the plasma potential at the position of the probe tip. The presented results for the spatial structure of the discharge are for value of the probe bias in the ion and electron saturation regions of the probe characteristics (respectively, U_{pr} = -80 V and a value of about 10 V above the plasma potential U_{pl}) as well as for probe bias equal to the floating potential U_{fl} and to the plasma potential U_{pl} as remarkable values on the probe characteristics. Showing results for $U_{\text{pr}} = U_{\text{fl}}$ permits separation — in the discussions — of effects of the probe (with its holder) immersed as a body into the discharge from effects of the bias applied to the probe tip.

Since the discussion is on the modifications in the discharge structure caused by inserting a probe in the discharge, the results are for the relative deviation of the plasma parameters from their values without a probe in the discharge:

$$\frac{\Delta\Theta_k}{\Theta_k} = \frac{(\Theta_k)_{\text{with probe}} - (\Theta_k)_{\text{w/o probe}}}{(\Theta_k)_{\text{w/o probe}}}, \tag{9}$$

where with Θ_k, the electron density n_e and temperature T_e and the plasma potential Φ are denoted. The consecutive modifications in the discharge when the probe is moved deeper in it are discussed based on results for three axial positions of the probe: z_{pr} = 2, 5 and 8 cm. A probe position (z_{pr} = 10 cm) very close to the back wall of the discharge, also discussed, determines completely different spatial structure of the deviations in the plasma parameters. Influence of the gas pressure is briefly commented on via results for p = 50 mTorr.

Figure 2 shows a typical structure of a discharge inductively driven by a planar coil, obtained without a probe immersed in it. It is characterizes with high electron temperature T_e in the rf power deposition region and a maxima of the electron density n_e and of the plasma potential Φ in its vicinity. The remote plasma region outside it shows up with the decrease in T_e, n_e and Φ.

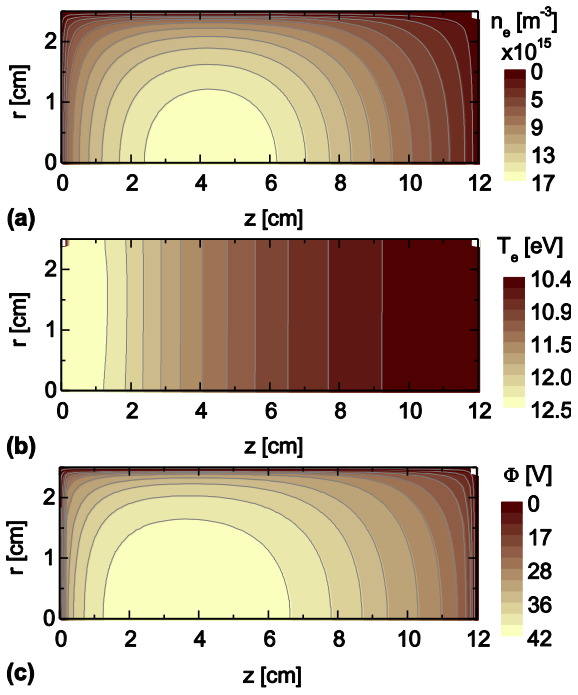

FIG. 2. Spatial distribution of the electron density (a) and temperature (b) and of the plasma potential Φ (c) without a probe inserted in the discharge; gas pressure p = 10 mTorr.

Figures 3-7 present the deviations in the spatial distribution of n_e, T_e, and Φ caused by the probe, together with its holder. On the figures, the probe is located at $r = 0$ (as shown in Fig. 1) and it is moved inside the discharge along the z-axis starting from $z = 0$; z_{pr} marks the position of the probe tip. Results obtained with a probe immersed into the discharge are compared with those (Fig. 2) without a probe and the relative deviations (9) are presented. Positive $\Delta\Theta_k/\Theta_k$ means that the local value of the given plasma parameter obtained with a probe immersed in the discharge is higher than that without a probe; negative $\Delta\Theta_k/\Theta_k$ means the opposite.

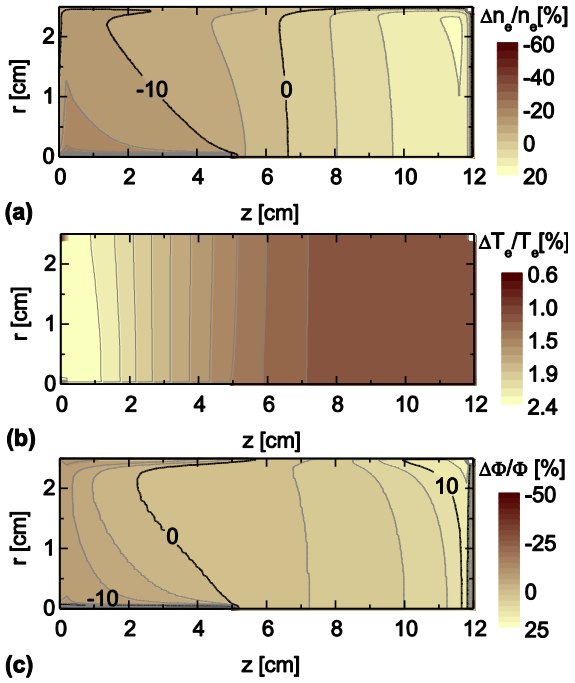

FIG. 3. Relative deviations in the spatial distribution of the electron density $\Delta n_e/n_e$ and temperature $\Delta T_e/T_e$ and of the plasma potential $\Delta\Phi/\Phi$ caused by the probe: axial position of the probe $z_{pr} = 5$ cm and probe bias equal to the floating potential ($U_{pr} = U_{fl} = 19.5$ V); $p = 10$ mTorr.

Figure 3 shows the results in the case when the probe is biased at the floating potential. Since in this case the electron and ion fluxes to the tip of the probe are equal as on the dielectric wall of its holder, the changes in the spatial distribution of the plasma parameters are, in fact, modifications in the discharge structure caused by a probe (together with its holder) immersed as a body into the discharge. Due to the addition wall losses of charged particles mainly on the surface of the probe holder, which is quite larger than that of the probe tip, the electron temperature T_e increases in the entire discharge volume (Fig. 3(b)). The highest relative increase of T_e (up to 2.4%) is in the discharge volume extended over a distance in the z-direction approaching the length of the probe holder, i.e. it is behind the probe tip. The T_e-increase, leading to an increased charged particle production, comes to compensate the increased losses in the discharge due to the radial flux of the ions to the

probe holder (and to the probe tip). The changes in the spatial distribution of the ion density $n_i = \sum_{j=1}^{3} n_j$, due to the radial ion losses, influence the spatial distribution of the electron density n_e, (because of its relation to n_i via the condition of quasi-neutrality) and of the plasma potential Φ, due to its relation to the charged particle accumulation in the discharge.

Whereas the spatial distribution of T_e (Fig. 3(b)) is more or less homogeneous in the radial direction (due to the high thermal conductivity at low gas pressure), the deviations of the electron density n_e show up with well pronounced radial structure (Fig. 3(a)). The lower values of $\Delta n_e/n_e$ are sticked close to the probe holder and to the side wall of the discharge as shown by the (-10%)-contour in Fig. 3(a). Starting with the value of -10% of $\Delta n_e/n_e$ at the position of the probe tip, the deviation in the spatial distribution of n_e becomes stronger towards $z = 0$, i.e., in the discharge region where the probe holder is inserted, reaching its highest (in magnitude) value in the sheath around the probe holder. The positions with the same values of n_e without and with a probe in the discharges, marked by the zero-contour in Fig. 3(a), are followed by an increase in n_e towards the back wall of the discharge at $z = 12$ cm. The deviations in the spatial distribution of the plasma potential Φ (Fig. 3(c)) caused by the probe, being weaker than those of n_e, are in the same trends. However, the (-10%)-contour of $\Delta\Phi/\Phi$ is strongly sticked to the probe holder, i.e., the strong decrease of Φ is locked in the probe sheath and in the wall sheath around the probe holder. The value of Φ at the position of the probe tip is almost the same without and with a probe in the discharge and the region with deviations higher than 10% is pressed to the back wall of the discharge.

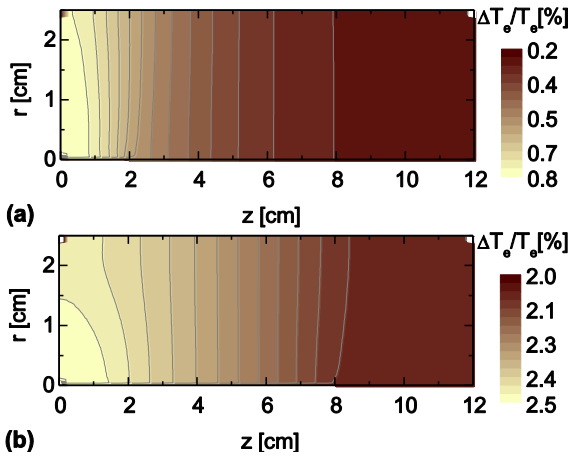

FIG. 4. Relative deviations in the spatial distribution of electron temperature $\Delta T_e/T_e$ obtained for different positions of a probe biased at the floating potential: (a) $z_{pr} = 2$ cm and (b) $z_{pr} = 8$ cm; $p = 10$ mTorr.

Figures 4 and 5 together with Figs. 3(a) and 3(b) show the modifications in the spatial distribution of n_e and T_e when the probe is moved deeper into the discharge. The results in Figs. 4 and 5 are also for a probe biased at the floating potential ($U_{pr} = U_{fl}$), thus, showing like in Fig. 3, modifications due to a probe (together with its holder) immersed as a body into the discharge.

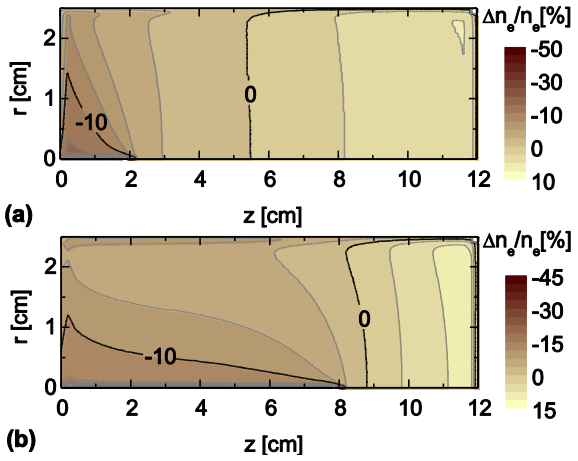

FIG. 5. The same as in Fig. 4, but for the electron density.

When the probe is moved deeper into the discharge (from $z_{pr} = 2$ cm till $z_{pr} = 8$ cm shown in Figs. 3-5), the additional wall at the discharge axis, which the probe holder appears to be, increases its surface. This leads to a shift of the interval of the electron temperature increase towards higher values (Fig. 3(b) and 4) and enlarges the extension (along the z-axis) of the region of the T_e-increase. In fact, the latter moves inside the discharge together with the probe advance. The comparison of Fig. 3(a) with Figs. 5(a) and 5(b) also shows the gradually increasing influence of the probe on the axial (and entire) discharge structure. Since the (-10%)-contour of $\Delta n_e/n_e$ starts always from the position of the probe tip, it moves deeper in the discharge together with the probe advance along z, leaving behind itself the discharge volume with stronger decrease of n_e in the vicinity of the probe holder. The zero-contour of $\Delta n_e/n_e$, which draws the positions of the same values of n_e as in a discharge without a probe is always in front of the probe tip. It also shifts deeper in the discharge together with the probe advance. The probe position $z_{pr} = 5$ cm (Fig. 3(a)) shows up with the highest increase of n_e in the region from the side of the back wall of the discharge. Because Q_{ext} is kept the same, probe positions $z_{pr} = 2$ cm and $z_{pr} = 8$ cm provide, respectively, too much and too less room for higher relative increase of n_e. Like in the case of $z_{pr} = 5$ cm (Fig. 3(c)), the modifications in the spatial distribution of Φ at $z_{pr} = 2$ cm and $z_{pr} = 8$ cm are in the trend of those of n_e.

The bias applied to the probe tip introduces additional modifications in the entire discharge structure (Fig. 6 and 7 where 2D plots of the relative deviations $\Delta T_e/T_e$ and $\Delta n_e/n_e$ are shown for a probe position z_{pr} = 2 cm). The probe bias of U_{pr} = -80 V in Fig. 6(a) and Fig. 7(a) is in the ion saturation region of the probe characteristics whereas the bias of U_{pr} = 44.5 V in Fig. 6(b) and Fig. 7(b) is in the electron saturation region. The comparison with the spatial distribution of $\Delta T_e/T_e$ and $\Delta n_e/n_e$ in Figs. 4(a) and 5(a) also obtained for z_{pr} = 2 cm but at $U_{pr} = U_{fl}$ shows the additional ─ to the probe holder ─ modifications due to the probe bias.

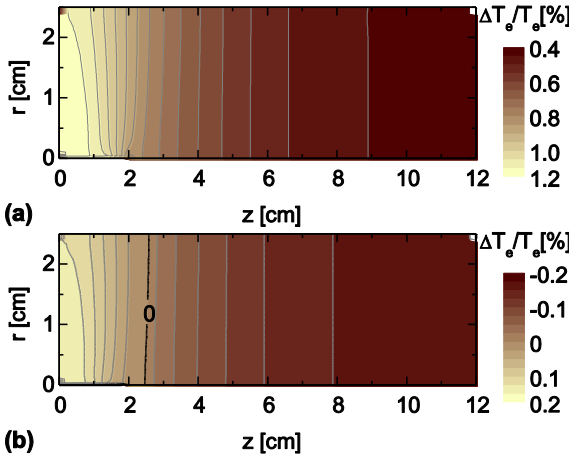

FIG. 6. Relative deviations in the spatial distribution of the electron temperature $\Delta T_e/T_e$ obtained at z_{pr} = 2 cm for different values of the probe bias: (a) U_{pr} = -80 V and (b) U_{pr} = 44.5 V; p = 10 mTorr.

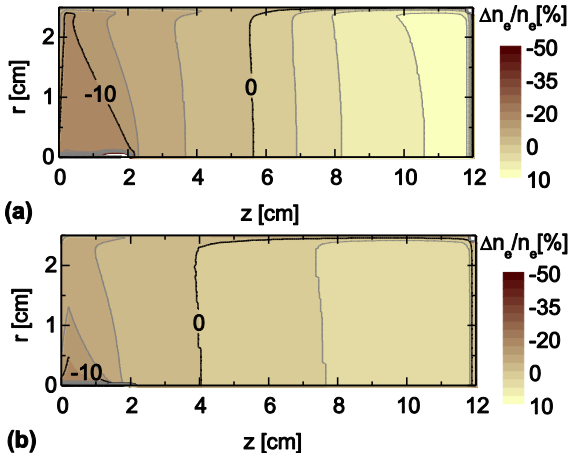

FIG. 7. The same as in Fig. 6, but for the electron density.

The higher ion losses at the probe tip surface due to the higher radial flux of the ions when the probe is biased at high ─ in magnitude ─ negative potential leads to higher increase of T_e (Fig. 6(a) compared to Fig. 4(a)): The interval of the changes

in T_e is shifted towards higher values and the region of the high T_e-increase is enlarged covering even z-positions in front of the probe tip. Respectively, the region with low n_e-values, marked by the (-10%)-contours in Figs. 7(a) and 5(a) is enlarged when the probe is negatively biased. In the opposite, a probe bias in the electron saturation region of the probe characteristics (Figs. 6(b) and 7(b)), diminishing the radial ion flux to the probe, reduces the ion losses. This leads to lowering of the electron temperature even below its value obtained without a probe in the discharge (Fig. 6(b)). The changes in T_e results in narrowing of the region with high reduction of n_e, marked by the (-10%)-contour in Fig. 7(b) (compared to Fig. 5(a)) and its sticking closer to the probe holder.

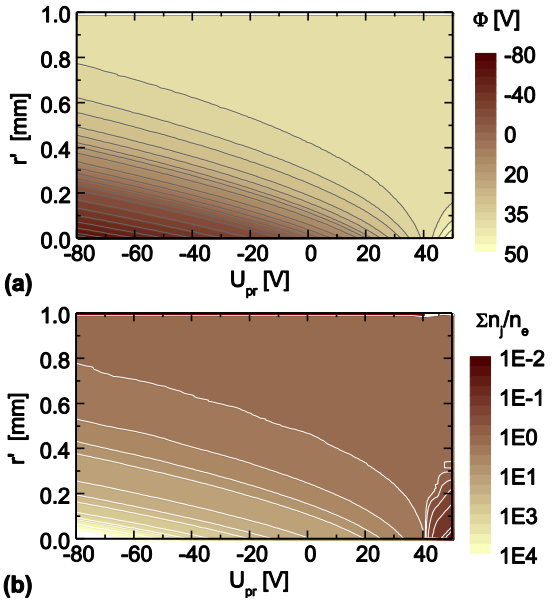

FIG. 8. 2D plots presenting the thickness of the probe sheath: radial variation of the plasma potential Φ (a) and of the ratio $\left(\sum_{j=1}^{3} n_j\right)/n_e$ of the ion and electron densities (b) with the changes of the bias U_{pr} applied to the probe positioned at z_{pr} = 5 cm. The presented radial variations are at z_{pr} = 4.7 cm, i.e. in the middle of the probe tip length and r' = 0 is on the probe surface.; p = 10 mTorr.

Figure 8, which shows the radial variation (at the z-position which is at the middle of the length of the probe tip) of the dc potential Φ and of the ratio $\left(\sum_{j=1}^{3} n_j\right)/n_e$ of the ion and electron densities for different values of the probe bias U_{pr}, displays very well the probe sheath and the variation of its thickness r_{sh} with changing the bias applied to the probe. The latter has been varied from U_{pr} = -80 V, i.e., from a value which is deep in the ion saturation region of the probe characteristic, till U_{pr} = 50 V, i.e., about 10 V above the plasma potential U_{pl}. The value of the latter (U_{pl} = 42 V, Fig. 8(a)) appears at the point

where the region of the unperturbed quasi-neutral plasma ($\left(\sum_{j=1}^{3} n_j\right)/n_e = 1$, Fig. 8(b)) touches the U_{pr}-axis in Figs. 8(a) and 8(b). The widening of the probe sheath with lowering the probe bias below U_{pl} which reminds an outspread fan appears in a correlated manner both on the Φ- and $\left(\sum_{j=1}^{3} n_j\right)/n_e$ - plots. Starting from a value of about r_{sh} = 0.8 mm at U_{pr} = -80 V, i.e., in the ion saturation region of the probe characteristics, the thickness of the sheath of uncompensated positive charge (Fig. 8(b)) around the probe reduces to a zero value at $U_{pr} = U_{pl}$, followed by formation of a sheath of uncompensated negative charge for $U_{pr} > U_{pl}$.

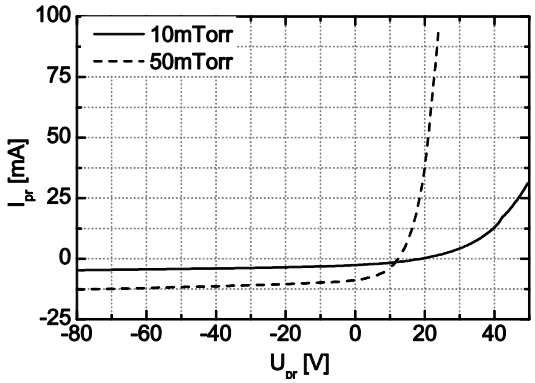

FIG. 9. Probe characteristics resulting from the model at p = 10 and 50 mTorr for z_{pr} = 3 cm.

Probe characteristics obtained from the model at z_{pr} = 3 cm are given in Fig. 9 as an example. The complete axial profiles of the plasma parameters ─ electron density and temperature and plasma potential ─ resulting from processing the probe characteristics are compared in Fig. 10 with the corresponding results obtained from the models without and with a probe in the discharge. The results from the model with a probe inserted in the discharge are at positions outside the probe sheath in front of the probe. As it has been already commented on in the discussions on Figs. 3-7, regardless of the influence of the probe on the entire discharge structure, the plasma parameters at the positions of the probe do not deviate too much from their values obtained for a discharge without a probe: the differences are within 3% and 5%, respectively, for the electron temperature and for the plasma potential and within about 10% for the electron density. The values of the electron density and temperature and of the plasma potential shown in Fig. 10 as results from the probe characteristics are also in comparatively good agreement with the results from the model of a discharge without a probe. Since the study does not touch discussions on the probe theories for determination of the electron density from the ion saturation current of the probe

characteristics, the values of the electron density in Fig. 10(a) are calculated from the probe current I_{e0} at $U_{pr} = U_{pl}$ according to

$$I_{e0} = e\Gamma_{e0}S_{pr} \tag{10}$$

where $\Gamma = (1/4)n_e\upsilon_{th,e}$ is the electron thermal flux and S_{pr} is the surface of the probe tip. Respectively, the value of plasma potential appears at the knee of the probe characteristic (Fig. 9, however in a semi-logarithmic scale) between its transition and electron-saturation regions. The electron temperature is determined, as always,[1-3] from the slope of the semi-logarithmic plot of the transition region of the probe characteristics:

$$T_e = \frac{e}{\kappa}\left(\frac{\Delta \ln I_e}{\Delta U}\right)^{-1}. \tag{11}$$

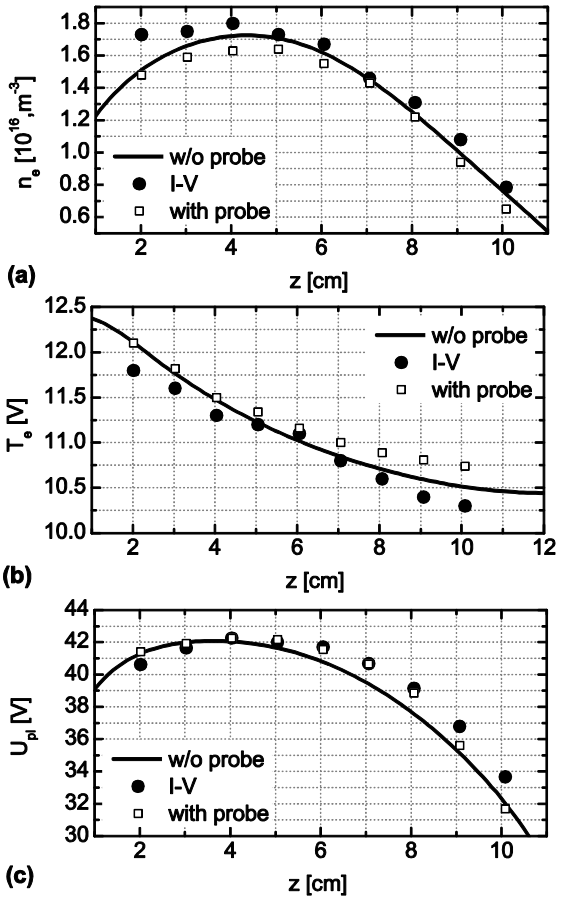

FIG. 10. Axial variation at the discharge axis (r = 0) of the electron density (a) and temperature (b) and of the plasma potential (c) obtained from the discharge models without (solid curve) and with (open squares) a probe inserted in the discharge. The results for the corresponding plasma parameters obtained by processing the probe characteristics are given by filled circles; p = 10mTorr.

Expression (11) results from the electron flux

$$\Gamma_e = \Gamma_{e0} \exp\left[\frac{e}{\kappa T_e}\left(U_{pr} - \Phi_{max}\right)\right] \tag{12}$$

in a retarding electric field (the field in the sheath around the probe) obtained, according to Ref. 18, from the Vlassov's approximation of the Boltzmann equation for the electron velocity distribution function. Figure 11 shows the very good agreement of the electron flux calculated according to (12) with the results for the electron flux from the plasma volume towards the probe surface provided by the model.

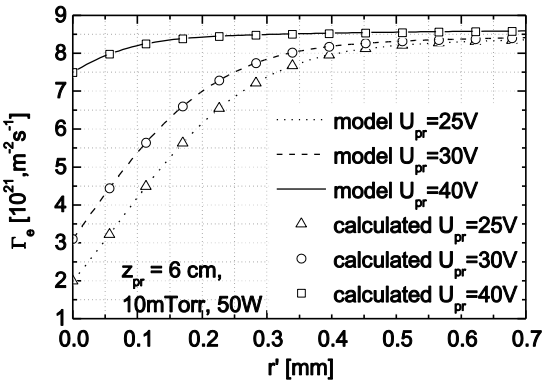

Fig. 11. Comparison of the results for the electron flux Γ_e in the probe sheath ($r' = 0$ is in the middle of the probe tip, at its surface) obtained from the model (curves) for three values of the probe bias U_{pr} ($U_{fl} < U_{pr} < U_{pl}$) with the results (symbols) calculated according to (12); z_{pr} = 6 cm and p = 10 mTorr.

Although the length of the discharge tube is 12 cm, the results for the structure of the discharge with a probe immersed in it shown in Figs. 3-7 are for probe positions up to z_{pr} = 8 cm. The reason is that for these positions the modifications in the spatial distribution of the plasma parameters go in the same trends when the probe is moved deeper into the discharge. The results in Fig. 12 show that the pattern changes when the probe is inserted too much deep into the discharge, at a position close to its back wall. The type of discharge does not change: It is the same as shown in Fig. 2 (a planar coil inductively driven discharge). However, the probe influences the discharge in a different manner, compared to the discharge modifications in Figs. 3-7. The location of the regions with high and low deviations in the values of n_e, T_e and Φ is opposite to that in Figs. 3-7. Whereas for $z_{pr} \leq 8$ cm n_e decreases on the side of the front wall of the discharge, i.e., in the region where the probe is inserted, for z_{pr} = 10 cm this region shows up with the highest relative increase of the electron density. The same

happens with the plasma potential Φ. The relative changes in T_e are also in the opposite: The stronger increase of T_e is in front of the probe (Fig. 12(b)), not behind it as for $z_{pr} \leq 8$ cm.

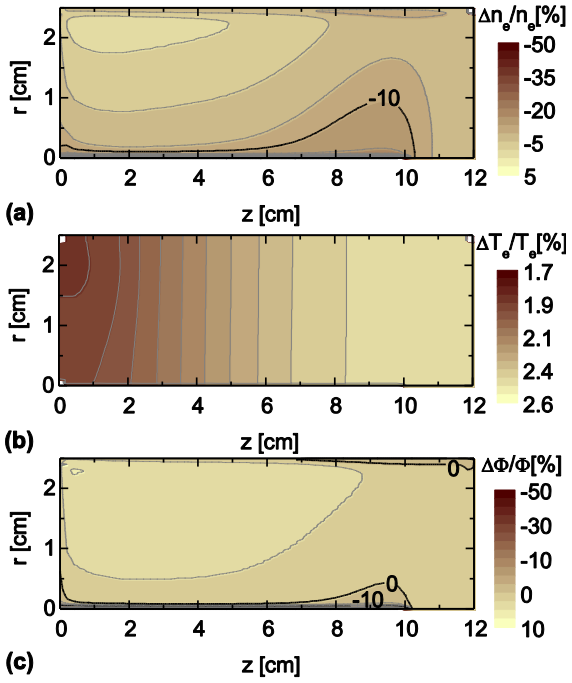

FIG. 12. Relative deviations in the spatial distribution of the electron density $\Delta n_e/n_e$ (a) and temperature $\Delta T_e/T_e$ (b) and of the plasma potential $\Delta\Phi/\Phi$ (c) for a probe positioned at z_{pr} = 10 cm. The probe is biased at the floating potential ($U_{pr} = U_{fl}$ = 17 V); p = 10 mTorr.

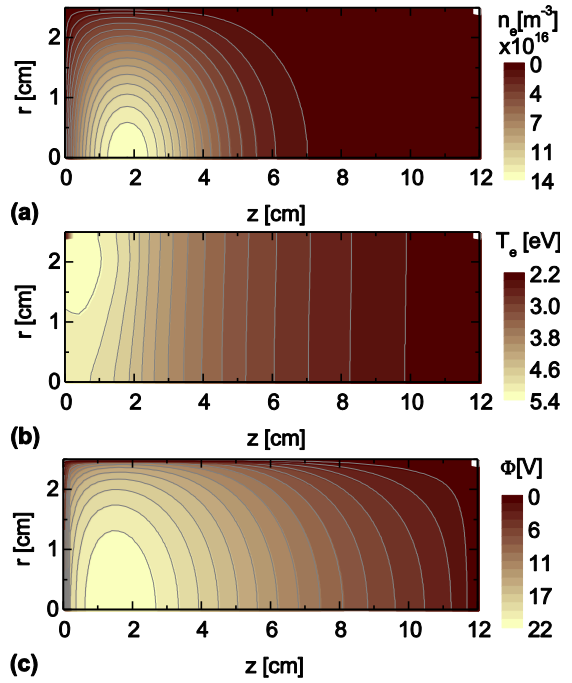

FIG. 13. Spatial distribution of the electron density (a) and temperature (b) and of the plasma potential (c) in a discharge without a probe in it, sustained at gas pressure p = 50 mTorr.

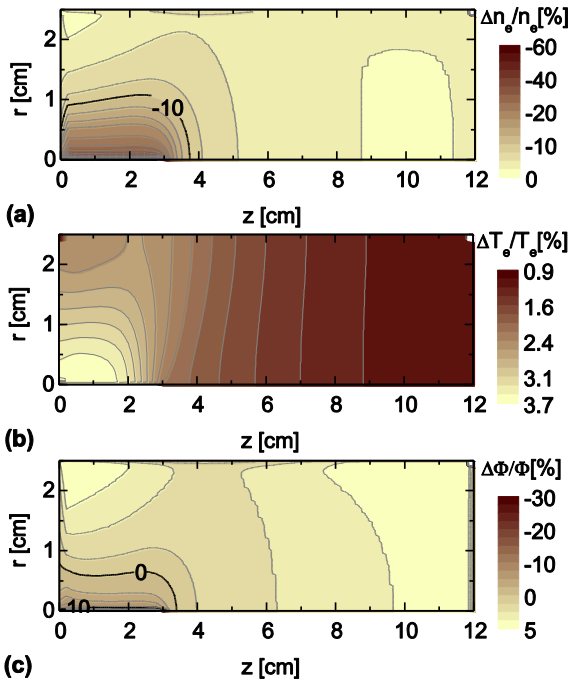

FIG. 14. Relative deviations in the spatial distribution of the electron density $\Delta n_e/n_e$ (a) and temperature $\Delta T_e/T_e$ (b) and of the plasma potential $\Delta\Phi/\Phi$ (c) caused by a probe inserted in a discharge sustained at p = 50 mTorr; probe position z_{pr} = 3 cm and probe bias at the floating potential ($U_{pr} = U_{fl}$ = 12 V).

Figure 13 and 14 shows results for a discharge sustained at a gas pressure p = 50 mTorr, i.e., at higher pressure compared to the discharges in Figs. 2-7. The spatial distributions of the plasma parameters n_e, T_e and Φ when there is no a probe inserted in the discharge are in Fig. 13, whereas the relative deviations in their distribution caused by the probe are in Fig. 14. In the latter case a probe positioned at z_{pr} = 3 cm is biased at the floating potential ($U_{pr} = U_{fl}$ = 12 V), i.e., the probe, and its holder, acts as a dielectric wall inserted around the discharge axis.

The discharge without a probe (Fig. 13) shows up as in Fig. 2, with its typical structure of an inductively driven discharge, with high T_e, n_e and Φ in the rf power deposition region (and its vicinity) and remote plasma region away from it. However, due to the reduced thermal conductivity when the gas pressure is higher, the region of high electron temperature is more localized which leads to stronger localization of the spatial distribution of the electron density. In general, the nonlocality of the discharge behavior is reduced, as it should be expected. The difference in the values of the plasma parameters compared to Fig. 2, is also as it should be expected for a discharge sustained at higher gas pressure. The electron temperature and plasma potential are lower (because of the lower losses of charged particles via their fluxes to the walls when the gas pressure is higher) and the electron density is higher (since under the conditions of lower losses the rf power input is kept the same). The probe characteristics in Fig. 9 also show the difference in the plasma parameters for

p = 10 mTorr and 50 mTorr. The steeper increase at p = 50 mTorr of the probe current in the transition region of the probe characteristics calls for lower T_e in this case. The obtained higher ion saturation current is due the higher plasma density.

In general, the relative deviations in the spatial distribution of the plasma parameters caused by a probe inserted in the discharge sustained at p = 50 mTorr follow the trends shown in Fig. 3 (for p = 10 mTorr): (i) The electron temperature increases over the entire discharge volume, more stronger in the discharge region axially extended over the length of the probe holder; (ii) The electron density and the plasma potential decrease in this region. However, the deviations caused by the probe are affected by the reduced nonlocality in the discharge behavior (Fig. 14 compared to Fig. 3). The relative increase of $\Delta T_e/T_e$ (Fig. 14(b)) is not anymore radially homogeneous and the reduction in n_e and Φ caused by the probe is localized stronger in the vicinity of the probe, and its holder.

IV. CONCLUSIONS

Langmuir probes are widely used in the plasma diagnostics, with the assumption that the plasma parameters outside the sheath around the probe are not influenced by the presentce of the probe in the discharge. The results from the 2D fluid-plasma model of a low-pressure discharge with a probe in it, presented in this study, show that the probe modifies the entire discharge structure, causing redistribution in the spatial variation of the electron density and temperature and of the plasma potential. The probe holder, acting as an additional wall inserted in the discharge, appears as a main reason for the changes in the spatial discharge structure. The bias applied to the probe tip leads to additional changes which are stronger at high negative potential applied to the probe, i.e., in the ion saturation region of the probe characteristics. The pattern of the spatial redistribution in the plasma parameters advances deeper inside the discharge together with the movement of the probe. Regardless of the modifications in the entire discharge volume the values of the plasma parameters at the position of the probe are not strongly influenced by its presence in the discharge. This is shown by comparison of results from models with and without a probe as well as by results for the plasma parameters obtained from of probe characteristics. The conclusions is that uncertainly of about 10% due to modification of the discharge structure by the probe should be added as an error when the accuracy in the determination of the plasma parameters from probe diagnostics is estimated.

ACKNOWLEDGMENTS

This work has been carried out within the framework of the EUROfusion Consortium and has received funding from the Euratom research and training programme 2014-2018 under grant agreement No 633053. The views and opinions expressed herein do not necessarily reflect those of the European Commission.

REFERENCES:

[1]R.H. Huddlestone and L.S. Leonard, eds., *Plasma Diagnostics Techniques* (Academic, New York, 1965).

[2]W. Lochite-Holtgreven, ed., *Plasma Diagnostics* (North-Holland, Amsterdam, 1968).

[3]M. L. Liberman and A. L. Lichtenberg, *Principles of Plasma Discharges and Material Processing* (Wiley, New York, 1994).

[4]J. E. Allen, R. L. Boyd, and P. Reynolds, Proc. Phys. Soc. **70**, 297 (1957).

[5]J. E. Allen, Physica Scripta **45**, 497 (1992).

[6]B. M. Annaratone, M. W. Allen, and J. E. Allen, J. Phys. D: Appl. Phys. **25**, 417 (1992).

[7]F. F. Chen, Phys. Plasmas **8**, 3029 (2001).

[8]F. F. Chen, Plasma Sources Sci. Technol. **18**, 035012 (2009).

[9]St. Lishev, Ts. Paunska, A. Shivarova, and Kh. Tarnev, Rev. Sci. Instrum. **83**, 02A702 (2012).

[10]D. Yordanov and St. Lishev, *Proceedings of the 32nd International Conference on Phenomena in Ionized Gases*, Iaşi, Romania, 26th-31st July 2015, P1.04.

[11]St. Lishev, D. Iordanov, Kh. Tarnev, and A. Shivarova, *Proceedings of the 31st International Conference on Phenomena in Ionized Gases*, Granada, Spain, 14th-19th July 2013, topic number: 8.

[12]St. Lishev, D. Yordanov, and A. Shivarova, Rev. Sci. Instrum. **85**, 02B101 (2014).

[13]D. Yordanov, St. Lishev, and A. Shivarova, Rev. Sci. Instrum. **87**, 02B116 (2016).

[14]Ts. Paunska, A. Shivarova, Kh. Tarnev and Ts. Tsankov, Phys. Plasmas **18**, 023503 (2011).

[15]St. St. Lishev, A.P. Shivarova, and Kh. Ts. Tarnev, J. Plasma Phys. **77**, 469 (2011).

[16]J. P. Boeuf and L. C. Pitchford, Phys. Rev. E **51**,1376 (1996).

[17]G. Y. M. Hagelaar, F. J. de Hoog, and G. M. W. Kroesen, Phys. Rev. E **62**, 1452 (2000).

[18]V. L. Granovskiy, *Electrical Current in Gases* (Nauka, Moscow, 1971), in Russian.